# Laser Absorption in Relativistically Underdense Plasmas by Synchrotron Radiation

C. S. Brady,[1] C. P. Ridgers,[2] T. D. Arber,[1] A. R. Bell,[2] and J. G. Kirk[3]
[1]Physics Department, University of Warwick, Coventry CV4 7AL, United Kingdom
[2]Clarendon Laboratory, University of Oxford, Parks Road, Oxford OX1 3PU, United Kingdom
[3]Max-Planck-Institut für Kernphysik, Postfach 10 39 80, 69029 Heidelberg, Germany
(Received 13 March 2012; published 14 December 2012)

A novel absorption mechanism for linearly polarized lasers propagating in relativistically underdense solids in the ultrarelativistic ($a \sim 100$) regime is presented. The mechanism is based on strong synchrotron emission from electrons reinjected into the laser by the space charge field they generate at the front of the laser pulse. This laser absorption, termed reinjected electron synchrotron emission, is due to a coupling of conventional plasma physics processes to quantum electrodynamic processes in low density solids at intensities above $10^{22}$ W/cm$^2$. Reinjected electron synchrotron emission is identified in 2D QED-particle-in-cell simulations and then explained in terms of 1D QED-particle-in-cell simulations and simple analytical theory. It is found that between 1% (at $10^{22}$ W/cm$^2$) and 14% (at $8 \times 10^{23}$ W/cm$^2$) of the laser energy is converted into gamma ray photons, potentially providing an ultraintense future gamma ray source.

DOI: 10.1103/PhysRevLett.109.245006 PACS numbers: 52.38.Dx, 52.38.Ph, 52.65.Rr

With the application of chirped pulse amplification to optical laser systems [1,2], laser power has increased dramatically in the last few decades. As a result, next generation 10 PW lasers ($I > 10^{23}$ W cm$^{-2}$) [3] will generate electromagnetic waves of such large amplitude that on interaction with matter they generate an entirely new plasma state—an ''ultrarelativistic plasma''. In such a plasma, the laser accelerates the electrons to Lorentz factors $\gamma \gg 1$. Ultrarelativistic plasmas have many exciting applications, potentially finding uses as a tabletop synchrotron light source or in the generation of dense electron-positron plasmas [1]. In addition, conventional applications of relativistic plasmas such as: fast ignition inertial confinement fusion [4], ion-acceleration to multi-GeV energies for medical applications [5], and high-harmonic generation to create attosecond pulses [6], must be revisited in the ultrarelativistic regime. Despite this, the physics of ultrarelativistic plasmas remains largely unexplored.

Synchrotron radiation from an electron accelerated by the laser's electric fields is controlled by the parameter $\eta = (\gamma/E_s)|\mathbf{E}_\perp + \boldsymbol{\beta} \times c\mathbf{B}|$ [7]. $E_s = 1.3 \times 10^{18}$ V m$^{-1}$ is the Schwinger field required to break the vacuum down into electron-positron pairs [8] and $\mathbf{E}_\perp$ is the component of the laser's electric field perpendicular to the electron's motion. As $\eta$ approaches unity, synchrotron radiation becomes important in the plasma energetics [9]. Assuming $\gamma \approx a$, this amounts to $\gamma > 100$. $\eta \approx 1$ is also when quantum corrections to the classical synchrotron spectrum [7] must be included. The most important correction is the reduction in the power radiated by each electron below the classical prediction by a factor $g(\eta)$ [7,9] (analogous to the Gaunt factor). The emitted synchrotron gamma ray photons are sufficiently energetic that they can produce electron-positron pairs in the laser fields by the multiphoton Breit-Wheeler process [8,9]. The importance of these QED processes has lead to the ''ultrarelativistic'' plasma regime sometimes being referred to as the ''QED-plasma'' regime [1]. The most fruitful way of making detailed predictions of the behavior of these systems is large scale direct numerical simulation using methods such as QED-PIC which extend the Vlasov-Maxwell system to include the synchrotron radiation and pair production. The PIC code EPOCH [10] has been extended to include these effects [1] using the Monte Carlo model described in Duclous *et al.* [11]. This model was found in Ref. [11] to generate the correct synchrotron emission spectrum.

For a one micron laser, $\eta$ approaches unity when the laser intensity approaches $10^{22}$ W cm$^{-2}$ ($\gamma > 100$). This is also the condition for which solid-density plasmas become relativistically transparent. It is difficult to exactly define transparency at ultrarelativistic intensity since the pileup of density at the laser front means that the target density with which the laser interacts is not that of the undisturbed target [12] and the situation is further complicated for a linearly polarized electromagnetic wave as the Lorentz factor for the electron varies over the wave period and so one would expect the plasma to be both over and under dense at various points in the laser cycle. While transparency could be defined simply here as occurring when the laser frequency becomes greater than the relativistically-corrected plasma frequency $\omega_p^{\mathrm{rel}} = (n_e e^2/\gamma m_e \epsilon_0)^{1/2}$ (for a solid-density plasma of electron number density $n_e$), this is likely not to be particularly illuminating. As will be shown from simulations, there still exists a regime where the plasma is a few times relativistically underdense by this definition and the electrons and the ions decouple. The laser expels electrons from its focus but the ions remain behind and the laser is transmitted

 

through the target. This regime will be referred to as "relativistically underdense". Relativistically underdense plasmas can have densities many orders of magntiude greater than underdense plasmas typically investigated with optical lasers and therefore, new collective plasma effects can significantly affect the propagation of electromagnetic waves in these plasmas.

Gamma ray production in overdense [1] and nonrelativistically underdense plasmas [9] has been previously studied, but the behavior of a relativistically underdense (as defined above) target is not yet understood, although the work of Nakamura *et al.* [13] includes some of the dynamics of this regime. To understand this regime, uniform $CH_2$ plastic targets which are relativistically underdense, but of solid density, were simulated under illumination with linearly polarized 1.06 $\mu$m lasers of 30 fs pulse length of various intensities using 2D QED-PIC simulations and the efficiency and nature of photon production was analyzed. The simulations were of a domain of 20 $\mu$m by 20 $\mu$m with 2048 gridpoints in each direction with 128 particles per species per cell. Convergence of the Monte Carlo based algorithm has been confirmed for all results in the Letter. These simulations show that emission of gamma rays is not continuous, but occurs during discrete "breakdown events" where electrons from the front of the laser beam are rapidly accelerated backwards. This period is termed the "breakdown time" $\tau_{bd}$ and the fact that the dynamics are dominated by these backwards acceleration events leads us to name the process reinjected electron synchrotron emission (RESE). Details of the first breakdown event are shown in Figs. 1(a) and 1(b) showing that photon production occurs only after the breakdown and that the photons are produced behind the laser front. Since the photons are produced by electrons traveling towards the laser, the produced photons are also predominantly produced with a backwards velocity [see Fig. 1(c)]. This is qualitatively different to photon production in Ridgers *et al.* [1] and in Nakamura *et al.* [13] where photon production is expected to be mainly in a hollow cone around the forward laser axis. While the emission of photons is a QED process, the fact that photons are only produced during a breakdown event means that the breakdown events themselves must be classical plasma physics processes. It is found that the time between gamma ray emission events depends only on the laser intensity and the initial target density and is always longer than the laser period. Up to 15% of the laser energy can be converted into gamma rays by higher laser intensities. Simulations were performed to identify the role of preplasma on the target front and it was found to change the rate of gamma ray production for underdense solids by less than 2%. Since a preplasma on an overdense target provides a region of underdense plasma for the laser to interact with, the resulting gamma ray emission becomes a mixture of the results in Ridgers *et al.* and those in this Letter if the preplasma scale length is sufficiently long. So long as the laser pulse has a uniform intensity, pulse length is almost irrelevant to the efficiency of gamma ray production. So long as the

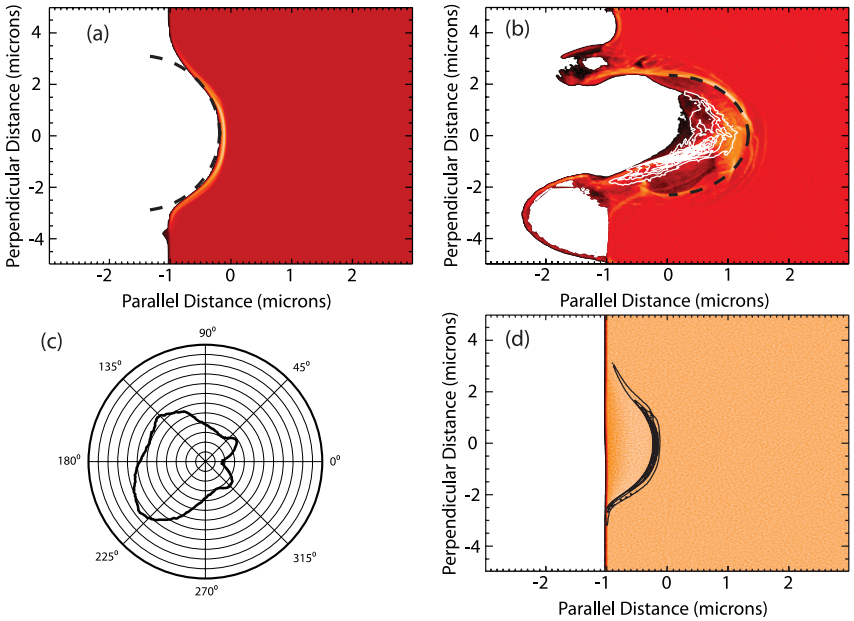


FIG. 1 (color online). Plots a) to c) are plots of the electron number density on a log scale with overlayed solid contour lines showing the location of the region of maximum photon production. a) is 1 fs before the first breakdown event, b) is 5 fs after the first breakdown event. The dashed line is the location of the head of the laser pulse. It is obvious that electrons behind the laser front produce the gamma ray emission. c) shows the angular distribution of the gamma rays. d) shows the ion density (solid colors) and the electron density (contour lines) at the breakdown event showing that ion and electron motion is decoupled. The perpendicular asymmetry in all plots is caused by the induced preferred direction from the direction of the electric field of the first laser cycle.

target is sufficiently thick, the breakdown events repeat for as long as the laser remains on, leading to a similar fraction of the total laser energy being converted into gamma rays. Pulses as long as 500 fs have been tested and show similar fractions of laser energy being converted to gamma rays as 30 fs pulses.

In Fig. 2, the energetics of the system are considered. The line marked "laser" shows that up to 15% additional laser absorption occurs above the absorption into fast electrons that would occur without QED effects. The line marked "gamma rays" shows that absorption is mostly accounted for by production of high energy photons. Generation of electron-positron pairs by the Breit-Wheeler process becomes more important as the laser intensity increases and up to 4% of the laser energy is converted into positron rest mass and kinetic energy at $8 \times 10^{23}$ W/cm$^2$. This explains why laser damping continues to increase with increasing laser intensity, whereas gamma ray energy reaches a peak of about 10% of laser energy at an intensity of $2 \times 10^{23}$ W/cm$^2$ and then decreases slightly at higher intensity. The symbols show that the results from 2D simulations match those from 1D simulations. The average photon energy is 1.1 MeV at $I = 10^{22}$ W/cm$^2$, rising to 32.1 MeV at $I = 8 \times 10^{23}$ W/cm$^2$. The ion energy increases in a manner similar to that observed by Chen *et al.* [14] and the electron energy decreases to conserve energy.

The mechanism is not hole boring as in Ref. [15], despite visual similarities. For relativistically underdense targets, the electron and ion dynamics decouple. This can be seen in several ways: the speed of the electron front as it propagates into the target at the head of the laser is not the relativistically correct hole boring speed, but is accurately modeled by the longitudinal speed of a relativistic free electron in a laser [16]. Secondly, rerunning the simulations with immobile ions makes little change to the final result unless the target density is near critical. For example, the photon production rate for a target of half corrected critical density changes by less than 1% if ion motion is ignored. Finally, in some parts of the parameter range considered, the decoupling of the ions and electrons is so complete that the ions have barely moved even when the first breakdown event occurs [see Fig. 1(d)]. Despite ions not being important to the details of this mechanism, similar results have been observed before in simulations relevant to ion acceleration, albeit usually as a secondary result. Schlegel *et al.* [17] identified electrons "leaking" through the head of a laser piston in underdense solids and being accelerated backwards by the space charge field and found that if radiation losses are included, a large fraction of the system energy is converted in gamma rays, although they did not connect the two effects and due to their not including QED corrections, they overestimated the gamma ray production. Tamburini *et al.* [18] identified that radiation reaction effects in relativistically underdense plasmas are more important for linearly polarized light than circularly polarized in situations where the laser doesn't burn through the target (such as considered here) and that electron backward motion is suppressed by radiation reaction effects, but consider that only in the context of it's influence on ion acceleration. Wave breaking is also unlikely to be the cause of the observed behavior. There is no evidence of Langmuir waves of an intensity above the wave breaking threshold observed in the simulations. If it is assumed that the breakdown time is the period of a Langmuir wave then no structure is seen on the length scale that would correspond to that period in plasma of the simulated density and temperature, furthering confidence that this process is not mediated by Langmuir waves. The breakdown event marks the time at which collective effects once again become important. 1D QED-PIC simulations were compared with the 2D simulations to identify the importance of multidimensional effects. It was determined that if the target density is high enough that transverse ponderomotive clearing of electrons from the laser bore is a slower process than the breakdowns, 1D and 2D simulations give similar results (see Fig. 2, comparing solid lines to open symbols). This allows us to formulate a 1D theory with confidence.

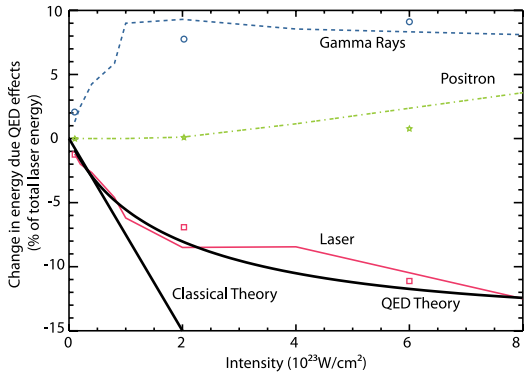


FIG. 2 (color online). Percentage change in energy components of the laser plasma system at different intensities. Lines are for 1D simulations. Squares are the laser energy, stars are positron energy, and circles are gamma rays from 2D simulations. The target densities in the 2D simulations are set so that the target is just relativistically underdense at the specified intensity, the 1D targets are all of density 0.16 g/cc. The solid line marked "QED theory" is the theoretical prediction given in this Letter with the corrected constant of proportionality. The solid line marked classical theory is the same calculation without the correction to the emission to to quantum effects, showing overprediction of emission.

This emission process, characterized by a "build-up" phase where the electrons are pushed forwards and a "breakdown" phase during which the electrons are reinjected into the laser pulse and emit, is further supported by Fig. 3. Figure 3(a) shows an electron phase space plot in the buildup phase at the same time as Fig. 1(a). At this time, the electrons are being pushed in the forwards direction.

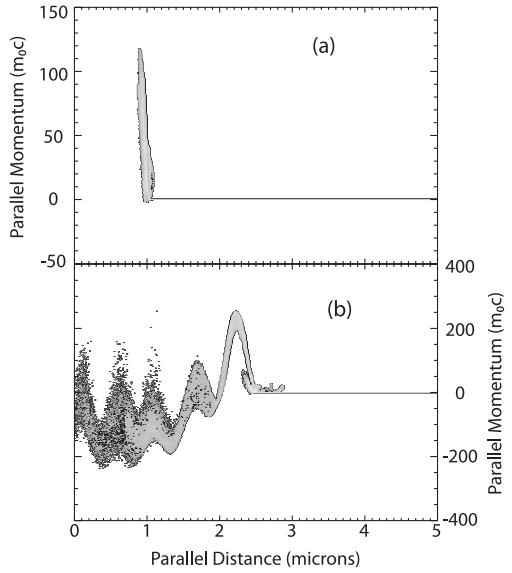


FIG. 3. Electron phase space plots for distance and momentum parallel to the laser axis a) just before the breakdown event and b) 5 fs after the breakdown event averaged over half a micron across the laser centreline of a 2D simulation with an intensity of $1 \times 10^{23}$ W/cm$^2$. The breadth of the momentum distribution for the backwards traveling electrons is due to QED radiation losses.

Figure 3(b) is the phase space plot after the breakdown corresponding to Fig. 1(c). To first approximation, the laser snowploughs the electrons ahead at speed $\approx c$ by the $\mathbf{v} \times \mathbf{B}$ force. The resulting charge separation between electrons and ions creates a strong longitudinal electric field, which after time $t$ is approximately $E_x(t) \simeq n_e ect/\epsilon_0$. Minimal synchrotron radiation occurs in this phase of the interaction as can be seen from the equation for $\eta$; the $\mathbf{E}_\perp$ is almost completely cancelled by the $\boldsymbol{\beta} \times \mathbf{B}$ term and $\eta \ll 1$. For a linearly polarized wave, the interaction enters a second phase. As the longitudinal field grows, it eventually exceeds the maximum in $\mathbf{v} \times \mathbf{B}$. When this occurs, the electron bunch is rapidly accelerated backwards and reinjected into the next peak in the laser's electric field. This will occur when $E_x = E_0$ (where $E_0$ is the peak laser electric field), i.e., after a time $\tau_{\rm bd} = \epsilon_0 E_0/(cen_e) = (n_{\rm cr}^{\rm rel}/n_e)(\tau_L/2\pi)$, where $\tau_L$ is the laser period. In this phase, $\eta \approx 2\gamma(t)E_\perp(t)/E_s$ and strong synchrotron emission and laser absorption occur. Here, $\gamma(t)$ is the (time-varying) Lorentz factor of the electrons and $E_\perp(t)$ is the laser field they experience as they move backwards. After the first bunch is reinjected, the laser pushes forwards another bunch of electrons at its head and the emission process repeats itself with periodicity equal to $\tau_{\rm bd}$.

To derive a scaling law for the absorption fraction to synchrotron radiation $f_{\rm abs}$, we assume that the electrons move at constant $\gamma(t) = a$ through a region of constant field $E_\perp(t) = E_0$ for a duration $\tau_L/2$ during the reinjection process. We assume the electron is then specularly reflected when it reaches the next maximum of the field and emission stops. The energy lost by the $N$ electrons picked up over time $\tau_{\rm bd}$ as they are reinjected is $\Delta E = NP\tau_L/2$. For laser focal spot size $A$ and electron number density $n_e$, $N = n_e A c t_{\rm bd}$. $P(\eta) = [4\pi\alpha_f m_e c^3 g(\eta)]/(3\lambda_c \eta^2)$ is the power radiated into synchrotron radiation by a single electron [19]; $\lambda_c$ is the Compton wavelength, $g(\eta)$ is the previously mentioned quantum-correction. If there are $N_{\rm bd} = \tau_{\rm PD}/\tau_{\rm bd}$ breakdown events during the laser pulse duration, $\tau_{\rm PD}$ the total energy emitted as gamma rays is $E_\gamma = N_{\rm bd}\Delta E$. The absorption fraction is given by $f_{\rm abs} = E_\gamma/E_{\rm las}$, where $E_{\rm las}$ is the total energy in the laser pulse. $E_\gamma = N_{\rm bd} NP\tau_L/2$ and $E_{\rm las} = \epsilon_0 E_0^2 Ac\tau_{\rm PD}$. Therefore, $f_{\rm abs} = C(\frac{a}{100})^2 n_{23}\lambda_{\mu\rm m} g(\eta)$, where $n_{23}$ is the electron number density in $10^{23}$ cm$^{-3}$ and $\lambda_{\mu\rm m}$ is the laser wavelength in microns. $C$ is a proportionality constant. For the choice of $\gamma(t) = a$ & $E_\perp(t) = E_0$, $C = 0.1$. While this scaling agrees well with simulations, $C$ must be reduced to $C = 0.06$ (see solid black line of Fig. 2). This is unsurprising, the simple model for $\gamma$ and $E_\perp$ provides an upper limit. In reality, the electrons will execute complicated trajectories when reinjected. The absorption equation shows that if $n_{23} = O(1)$ (as is only possible in solid-density underdense plasmas) then RESE absorption is important for $a > 100$, i.e., for intensities greater than $10^{22}$ W cm$^{-2}$. For $\eta \ll 1$ $g(\eta) \approx 1$ and $f_{\rm abs} \propto a^2$. For $\eta \gg 1$, $g(\eta) \approx 0.56\eta^{-4/3}$ and $f_{\rm abs} \propto a^{-2/3}$. These results also demonstrate the importance of using a QED correct formulation of synchrotron emission, since if this is not taken into account then at higher intensity, gamma ray emission is overestimated [see solid black line on Fig. 2(b) marked "Classical Theory"].

The new RESE absorption mechanism presented here is therefore important for understanding underdense ultrarelativisitic plasmas and converts laser energy into gamma rays with high efficiency, potentially leading to an ultrabright tabletop synchrotron source. Over the intensity range of lasers available in the next five years, RESE absorption will range from the detectable (1% absorption at $2 \times 10^{22}$ W/cm$^2$) to the dynamically crucial (15% absorption at $8 \times 10^{23}$ W/cm$^2$) and it's characteristic backwards propagation will allow easy experimental differentiation from other possible emission mechanisms. At the higher intensities in this range, a significant amount of laser energy is converted to electron-positron pairs. Therefore, RESE absorption in solid-density underdense plamas is among the most effective method for producing gamma rays and pairs with lasers available in the near-term.

[1] C. P. Ridgers, C. S. Brady, R. Duclous, J. G. Kirk, K. Bennett, T. D. Arber, A. P. L. Robinson, and A. R. Bell, Phys. Rev. Lett. **108**, 165006 (2012).

[2] P. Maine, D. Strickland, P. Bado, M. Pessot, and G. Mourou, IEEE J. Quantum Electron. **24**, 398 (1988).

[3] G. A. Mourou, C. L. Labaune, M. Dunne, N. Naumova, and V. T. Tikhonchuk, Plasma Phys. Controlled Fusion **49**, B667 (2007).
[4] M. Tabak, J. Hammer, M. E. Glinsky, W. L. Kruer, S. C. Wilks, J. Woodworth, E. M. Campbell, M. D. Perry, and R. J. Mason, Phys. Plasmas **1**, 1626 (1994).
[5] B. M. Hegelich, B. J. Albright, J. Cobble, K. Flippo, S. Letzring, M. Paffett, H. Ruhl, J. Schreiber, R. K. Schulze, and J. C. Fernández, Nature (London) **439**, 441 (2006).
[6] B. Dromey *et al.*, Nat. Phys. **2**, 456 (2006).
[7] T. Erber, Rev. Mod. Phys. **38**, 626 (1966).
[8] J. Schwinger, Phys. Rev. **82**, 664 (1951).
[9] A. R. Bell and J. G. Kirk, Phys. Rev. Lett. **101**, 200403 (2008).
[10] C. S. Brady and T. D. Arber, Plasma Phys. Controlled Fusion **53**, 015001 (2011).
[11] R. Duclous, J. G. Kirk, and A. R. Bell, Plasma Phys. Controlled Fusion **53**, 015009 (2011).
[12] F. Cattani, A. Kim, D. Anderson, and M. Lisak, Phys. Rev. E **62**, 1234 (2000).
[13] T. Nakamura, J. Koga, T. Esirkepov, M. Kando, G. Korn, and S. Bulanov, Phys. Rev. Lett. **108**, 195001 (2012).
[14] M. Chen, A. Pukhov, T.-P. Yu, and Z.-M. Sheng, Plasma Phys. Controlled Fusion **53**, 014004 (2011).
[15] A. P. L. Robinson, P. Gibbon, M. Zepf, S. Kar, R. G. Evans, and C. Bellei, Plasma Phys. Controlled Fusion **51**, 024004 (2009).
[16] J. N. Bardsley, B. M. Penetrante, and M. H. Mittleman, Phys. Rev. A **40**, 3823 (1989).
[17] T. Schlegel, N. Naumova, I. V. S. V. T. Tikhonchk, C. Labaune, and G. Mourou, Phys. Plasmas **16**, 083103 (2009).
[18] M. Tamburini, F. Pegoraro, A. D. Piazza, C. H. Keitel, and A. Macchi, New J. Phys. **12**, 123005 (2010).
[19] J. G. Kirk, A. R. Bell, and I. Arka, Plasma Phys. Controlled Fusion **51**, 085008 (2009).